

# Neutron-proton mass difference in isospin asymmetric nuclear matter

Ulf-G. Meißner<sup>1,2</sup>, A. M. Rakhimov<sup>3,4</sup>, A. Wirzba<sup>2</sup>, and U. T. Yakhshiev<sup>2,5</sup>

<sup>1</sup> Helmholtz-Institut für Strahlen- und Kernphysik (Theorie), D-53115, Universität Bonn, Germany

<sup>2</sup> Forschungszentrum Jülich, Institut für Kernphysik (Theorie), D-52425 Jülich, Germany

<sup>3</sup> Institute of Nuclear Physics, Academy of Sciences of Uzbekistan, Tashkent-132, Uzbekistan

<sup>4</sup> Institute of Physics and Applied Physics, Yonsei University, Seoul, 120-749, Korea

<sup>5</sup> Physics Department and Institute of Applied Physics, National University of Uzbekistan, Tashkent-174, Uzbekistan

Received: date / Revised version: date

**Abstract.** Isospin-breaking effects in the baryonic sector are studied in the framework of a medium-modified Skyrme model. The neutron-proton mass difference in infinite, asymmetric nuclear matter is discussed. In order to describe the influence of the nuclear environment on the skyrmions, we include energy-dependent charged and neutral pion optical potentials in the  $s$ - and  $p$ -wave channels. The present approach predicts that the neutron-proton mass difference is mainly dictated by its strong part and that it strongly decreases in neutron matter.

**PACS.** 12.39.Fe Chiral Lagrangians – 13.40.Gp Electromagnetic form factors – 21.65.+f Nuclear matter

## 1 Introduction

The medium dependence of isospin-breaking effects belongs to one of the fundamental questions in nuclear physics [1, 2, 3]. In particular, the neutron-proton mass difference in nuclear matter  $\Delta m_{np}^*$  is an interesting topic of nuclear astrophysics relevant to the evolution of the universe at an early stage [4, 5]. Furthermore, it is also important for the description of the properties of mirror nuclei [6], the stability of drip-line nuclei [7] and the transport in neutron-rich matter induced by heavy-ion collisions [8]. Although there exist various publications dealing directly with the density dependence of the neutron-proton mass difference [9, 10, 11, 12, 13, 14, 15, 16, 17] and its implications for asymmetric nuclear matter and finite nuclei properties [18, 19, 20, 21, 22, 23, 24, 25, 26, 27, 28, 29, 30, 31, 32], this quantity is still not well understood. Quantitatively and even qualitatively the predictions about the behavior of the neutron-proton mass difference in nuclear matter change from model to model.

Skyrme-soliton models have the inherent advantage compared with other hadronic models that they are based on chiral input and that they treat the properties and interactions of the nucleons on an equal footing [33, 34]. In this context we recently studied isospin-breaking effects in the baryonic sector of a medium-modified Skyrme model [35], by focusing on the single hadron properties in the nuclear environment rather than on the properties of the system as a whole. The approach predicted that the neutron-proton mass difference changes in an isospin-symmetric nuclear environment by a very small amount.

The isospin-breaking leading to this result was only due to a modification of the mesonic sector of the Skyrme model, originally introduced to generate the strong neutron-proton mass splitting in free space (in addition to the electromagnetic one) [36]. However, when the nucleons are embedded in an isospin-asymmetric environment, *additional* medium effects can be expected. To evaluate the latter in the present work we will consider the nucleon properties in homogeneous, infinite and isospin-asymmetric nuclear matter. The Lagrangian of the present study is a generalization of the in-medium Skyrme-type Lagrangian of Ref. [35]. In addition to the strong isospin-breaking in the mesonic sector it *explicitly* takes into account the different influences of the isospin-asymmetric environment on the charged ( $\pi^\pm$ ) and neutral ( $\pi^0$ ) pion fields via a built-in energy dependence in the  $s$ -wave pion-nucleon ( $\pi^\pm N$ ) scattering lengths [37, 38, 39, 40, 41] and the  $p$ -wave optical potential [42]. This additional energy dependence also alters the predictions for iso-symmetric matter considerably.

The paper is organized as follows: In Sect. 2 we formulate the model including the optical potential input and medium modifications. Section 3 discusses the classical Lagrangian and the pertinent equation of motion. In Sect. 4 we present the quantization procedure and the final expressions for the the strong and electromagnetic part of the in-medium neutron-proton mass difference. The results of the calculation are reported and discussed in Sect. 5. In Sect. 6 our conclusions are summarized and an outlook to future studies is given. Moreover, for clarification, two appendices are added. In the first one, we

discuss in detail the setup of the classical equation of motion in the presence of isospin-breaking terms. The second appendix is devoted to peculiarities in the construction of the charges and magnetic moments.

## 2 Formulation of the problem

### 2.1 Medium modification of the model

As in our previous work [35], we start with a generalized Skyrme-type Lagrangian which incorporates an explicit isospin-breaking term in the mesonic sector:

$$\mathcal{L} = \mathcal{L}_2 + \mathcal{L}_4 + \mathcal{L}_{\text{g}\chi\text{SB}}, \quad (1)$$

$$\mathcal{L}_2 = -\frac{F_\pi^2}{16} \text{Tr} (L_\mu L^\mu), \quad (2)$$

$$\mathcal{L}_4 = \frac{1}{32e^2} \text{Tr} [L_\mu, L_\nu]^2, \quad (3)$$

$$\mathcal{L}_{\text{g}\chi\text{SB}} = -\frac{F_\pi^2}{16} \left\{ \text{Tr} [(U - 1) \mathcal{M}_+^2 (U^\dagger - 1)] - \text{Tr} [(U - 1) \tau_3 \mathcal{M}_-^2 (U^\dagger - 1) \tau_3] \right\}, \quad (4)$$

where Einstein's summation convention is always assumed (if not specified otherwise).  $L_\mu = U^\dagger \partial_\mu U$  is given in terms of the chiral  $SU(2)$  matrix  $U = \exp(2i\tau_a \pi_a / F_\pi)$ , where  $\pi_a$  ( $a = 1, 2, 3$ ) are the Cartesian isospin-components of the pion field.  $F_\pi = 2f_\pi$  is the pion-decay constant, while  $e$  is the dimensionless Skyrme constant. Finally,  $\mathcal{M}_\pm \equiv \sqrt{(m_{\pi^\pm}^2 \pm m_{\pi^0}^2)/2}$  is defined in terms of the masses of the charged and neutral pions. As in Ref. [35] we insist on reproducing the empirical (isospin-averaged) masses of the nucleon and delta,  $m_N = 938$  MeV and  $M_\Delta = 1232$  MeV, in free space (density  $\rho = 0$ ) and without isospin breaking term ( $\mathcal{M}_- = 0$ ). Furthermore, as input for the free mass of the neutral pion we take the PDG-value [43]:  $m_{\pi^0} = 134.977$  MeV. These choices induce the values  $F_\pi = 108.11$  MeV and  $e = 4.826$ . Following Ref. [35] the mass of the charged pions  $m_{\pi^\pm}$  is extracted as a variational parameter  $m_{\pi^\pm} = 135.015$  MeV from the fit to the empirical value  $\Delta m_{\text{np}}^{(exp)} = 1.29$  MeV of the neutron-proton mass splitting in free space. Note that the dominant electromagnetic contribution to  $m_{\pi^\pm} - m_{\pi^0}$  is beyond the scope of the model.

The generalized pion mass term (4), which was originally proposed by Rathske [36], can be rewritten as

$$\mathcal{L}_{\text{g}\chi\text{SB}} = -\frac{F_\pi^2}{16} \left\{ \text{Tr} [(U - 1) m_{\pi^0}^2 (U^\dagger - 1)] + \sum_{a=1}^2 \text{Tr} (\tau_a U) \mathcal{M}_-^2 \text{Tr} (\tau_a U^\dagger) \right\}, \quad (5)$$

which is convenient for our up-coming modifications. When the pion fields are small,

$$U = \exp \left\{ \frac{2i\boldsymbol{\tau} \cdot \boldsymbol{\pi}}{F_\pi} \right\} \approx 1 + \frac{2i\boldsymbol{\tau} \cdot \boldsymbol{\pi}}{F_\pi} + \dots, \quad (6)$$

the Lagrangian (1) reduces to the Lagrangian for free pion fields

$$\mathcal{L}_{\text{low}} = \partial_\mu \pi^+ \partial^\mu \pi^- - \pi^+ m_{\pi^\pm}^2 \pi^- + \frac{1}{2} (\partial_\mu \pi^0 \partial^\mu \pi^0 - \pi^0 m_{\pi^0}^2 \pi^0), \quad (7)$$

$$\pi^\pm = \frac{1}{\sqrt{2}} (\pi_1 \mp i\pi_2), \quad \pi^0 = \pi_3. \quad (8)$$

In the medium the analog of the Lagrangian (7) reads

$$\begin{aligned} \mathcal{L}_{\text{low}}^* &= \frac{1}{2} \sum_{\lambda=\pm,0} \{ \partial_\mu \pi^{\lambda\dagger} \partial^\mu \pi^\lambda - \pi^{\lambda\dagger} (m_{\pi^\lambda}^2 + \hat{H}^\lambda) \pi^\lambda \} \\ &= \mathcal{L}_{\text{low}} - \frac{1}{2} \left\{ \pi_a \hat{H}^0 \pi_a + i\varepsilon_{ab3} \pi_a \Delta \hat{H} \pi_b \right\}, \end{aligned} \quad (9)$$

where  $\hat{H}^0$  and  $\Delta \hat{H}$  are linear combinations of the self energies of the charged pions:

$$\begin{aligned} \hat{H}^0 &= \frac{1}{2} (\hat{H}^- + \hat{H}^+), \\ \Delta \hat{H} &= \frac{1}{2} (\hat{H}^- - \hat{H}^+). \end{aligned} \quad (10)$$

As in Ref. [35] the medium-modified version (always marked by an asterix) of the Lagrangian (1), can be defined as

$$\mathcal{L} \rightarrow \mathcal{L}^* = \mathcal{L}_2 + \mathcal{L}_4 + \mathcal{L}_{\text{g}\chi\text{SB}}^*, \quad (11)$$

where for the general case of asymmetric matter  $\mathcal{L}_{\text{g}\chi\text{SB}}^*$  is given by formula<sup>1</sup>

$$\begin{aligned} \mathcal{L}_{\text{g}\chi\text{SB}}^* &= -\frac{F_\pi^2}{16} \left\{ \text{Tr} [(U - 1) (m_\pi^2 + \hat{H}^0) (U^\dagger - 1)] \right. \\ &\quad + \sum_{a,b=1}^2 \text{Tr} (\tau_a U) \left[ \delta_{ab} \mathcal{M}_-^2 \right. \\ &\quad \left. \left. + i\varepsilon_{ab3} \Delta \hat{H} / 2 \right] \text{Tr} (\tau_b U^\dagger) \right\}. \end{aligned} \quad (12)$$

It is easy to check that the Lagrangian (11) reduces to the Lagrangian (9) for the expansion (6) as well as to the medium-modified Lagrangian of Ref. [35] for the case of isospin-symmetric matter,  $\hat{H}^+ = \hat{H}^- = \hat{H}^0$  (in the parameterization of Ref. [35]).

### 2.2 Parameterization of the optical potentials

The polarization operators of the charged pions can be expressed in terms of energy-dependent pion-nucleus optical potentials [42] as follows:

$$\begin{aligned} \hat{H}_s^\pm(\omega, \mathbf{r}) &= -4\pi b^\pm(\omega, \mathbf{r}) \equiv \chi_s^\pm(\omega, \mathbf{r}), \\ \hat{H}_p^\pm(\omega, \mathbf{r}) &= \boldsymbol{\nabla} \frac{4\pi c^\pm(\omega, \mathbf{r})}{1 + 4\pi g' c^\pm(\omega, \mathbf{r})} \cdot \boldsymbol{\nabla} - \frac{4\pi\omega}{2m_N} (\boldsymbol{\nabla}^2 c^\pm(\omega, \mathbf{r})) \end{aligned} \quad (13)$$

<sup>1</sup> From now on  $m_\pi$  stands for the mass of the neutral pion, i.e.  $m_\pi \equiv m_{\pi^0}$ .

$$\equiv \nabla \chi_{p,1}^{\pm}(\omega, \mathbf{r}) \cdot \nabla - \frac{\omega}{m_{\pi}} \chi_{p,2}^{\pm}(\omega, \mathbf{r}), \quad (14)$$

$$b^{\pm}(\omega, \mathbf{r}) \equiv \left( b_0^{\text{eff}}(\omega) \rho(\mathbf{r}) \mp b_1(\omega) \delta \rho(\mathbf{r}) \right) \eta, \quad (15)$$

$$c^{\pm}(\omega, \mathbf{r}) \equiv \left( c_0(\omega) \rho(\mathbf{r}) \mp c_1(\omega) \delta \rho(\mathbf{r}) \right) \eta^{-1}, \quad (16)$$

$$\rho(\mathbf{r}) = \rho_n(\mathbf{r}) + \rho_p(\mathbf{r}), \quad (17)$$

$$\delta \rho(\mathbf{r}) = \rho_n(\mathbf{r}) - \rho_p(\mathbf{r}), \quad (18)$$

$$\eta = 1 + m_{\pi}/m_N, \quad (19)$$

where  $\rho_n$  and  $\rho_p$  are the neutron and proton densities, respectively. Note that additional  $\nabla^2 \rho$  and  $\nabla^2 \delta \rho$  terms are included in the  $p$ -wave optical potential since they are needed for the description of realistic pion-nucleus scattering data [42].

The chiral expansion of the off-shell pion-nucleon scattering amplitudes at vanishing pion three-momentum leads to energy-dependent  $s$ -wave isoscalar and isovector scattering lengths,  $b_0(\omega)$  and  $b_1(\omega)$ , respectively. The quantities  $c_0(\omega)$  and  $c_1(\omega)$  are the corresponding  $p$ -wave scattering volumes, whereas  $b_0^{\text{eff}}(\omega)$  is the *effective* isoscalar scattering length (see Eq. (22)). The correlation parameter  $g'$ , which renormalizes the pion dipole susceptibility, is fixed at  $g' = 0.47$ .

Within the counting scheme of pion-nucleon chiral perturbation theory from Refs. [37,38] and based on input from these references  $b_0(\omega)$  and  $b_1(\omega)$  can be expressed at order  $\mathcal{O}(m_{\pi}^3)$  as [39,40]

$$\begin{aligned} b_0(\omega) &\approx \frac{1}{4\pi\eta} \left( \frac{\sigma_{\pi N} - \beta\omega^2}{f_{\pi,\text{ph}}^2} + \frac{3g_A^2 m_{\pi}^3}{16\pi f_{\pi,\text{ph}}^4} \right) \\ &\approx \frac{1.206 m_{\pi}^{-1}}{4\pi\eta} (1 - m_{\pi}^{-2} \omega^2) \\ &\equiv -\frac{\tilde{b}_0}{4\pi\eta} (1 - m_{\pi}^{-2} \omega^2), \end{aligned} \quad (20)$$

$$\begin{aligned} b_1(\omega) &\approx -\frac{1}{4\pi\eta} \frac{\omega}{2f_{\pi,\text{ph}}^2} \left( 1 + \frac{\gamma\omega^2}{4\pi^2 f_{\pi,\text{ph}}^2} \right) \\ &\approx -\frac{1.115 m_{\pi}^{-1}}{4\pi\eta} (m_{\pi}^{-1} \omega + 0.143 m_{\pi}^{-3} \omega^3) \\ &\equiv \frac{\tilde{b}_1}{4\pi\eta} (m_{\pi}^{-1} \omega + 0.143 m_{\pi}^{-3} \omega^3). \end{aligned} \quad (21)$$

Here  $\sigma_{\pi N} = -4C_1 m_{\pi}^2 - 9g_A^2 m_{\pi}^3 / 64\pi f_{\pi,\text{ph}}^2 \approx 45$  MeV is the pion-nucleon sigma term, whereas the other parameters correspond to the “range term” [44,45,46]  $\beta = g_A^2 / 4m_N - 2C_2 - 2C_3 \approx 0.541 m_{\pi}^{-1}$  and also  $\gamma = (g_A \pi f_{\pi,\text{ph}} / m_N)^2 + \ln(2\Lambda_c / m_{\pi}) \approx 2.523$ . The axial-vector coupling constant  $g_A = 1.27$  and the pion decay constant  $f_{\pi,\text{ph}} = 92.4$  MeV are fixed to their empirical values, since they refer to the parameterization of the nuclear (matter) background. On the other hand, the parameter  $F_{\pi} = 2f_{\pi}$  of the Skyrme Lagrangian is fixed to the value 108.11 MeV, since this parameter together with  $e = 4.826$  and  $m_{\pi} = 134.977$  MeV refers to the soliton itself; *i.e.* the empirical (isospin-averaged) masses of the nucleon and delta are reproduced by this choice, as explained below Eq. (4). The value of the

cutoff-scale parameter  $\Lambda_c = 737$  MeV is adjusted to the threshold value of the isospin-odd on-shell  $\pi N$  scattering amplitude. The dimension-two low-energy constants  $C_{1,2,3}$  can be found *e.g.* in Refs. [37,38]. These values are consistent with the most recent pion-nuclei scattering data as it was summarized in Ref. [47] and lead to the threshold values  $b_0(m_{\pi}) \approx 0$  and  $b_1(m_{\pi}) \approx -0.0883 m_{\pi}^{-1}$ , respectively [48]. Within the errors these values of the scattering lengths are consistent with the more refined analysis of Ref. [49]. Furthermore, the incorporation of double scattering corrections in the  $s$ -wave pion polarization operator leads to the effective isoscalar scattering length

$$b_0^{\text{eff}}(\omega) \approx b_0(\omega) - \frac{3k_F}{2\pi} [b_0^2(\omega) + 2b_1^2(\omega)], \quad (22)$$

where  $k_F = [3\pi^2 \rho / 2]^{1/3}$  is the total Fermi momentum. The terms of higher order than  $\omega^2$  can be neglected in  $b_0^{\text{eff}}$  and  $b_1$ , provided that the condition  $\omega < m_{\pi}$  is met.<sup>2</sup>

For simplicity, we ignore the energy dependence in the  $p$ -wave scattering volumes and replace  $c_0(\omega)$  and  $c_1(\omega)$  by the constant threshold values  $c_0(m_{\pi}) = 0.21 m_{\pi}^{-3}$  and  $c_1(m_{\pi}) = 0.165 m_{\pi}^{-3}$  of the ‘current’ SAID analysis [50]. This is compatible with the discussion in Ref. [41]. Furthermore, all terms proportional to odd  $\omega$  powers in  $\hat{H}_p^0$  and even ones in  $\Delta \hat{H}_p$  are neglected. This is consistent with the remark in footnote 2 and the disregard of pion-absorption in this approach.

In summary, one can write the polarization operators (10) as follows:

$$\begin{aligned} \hat{H}_s^0 &= \frac{\chi_s^-(\omega) + \chi_s^+(\omega)}{2} \\ &\approx \left( \tilde{b}_0 + \frac{3k_F}{8\pi^2 \eta} \tilde{b}_0^2 \right) \rho - \left( \tilde{b}_0 + \frac{3k_F}{4\pi^2 \eta} (\tilde{b}_0^2 - \tilde{b}_1^2) \right) \rho \frac{\omega^2}{m_{\pi}^2} \\ &\equiv \chi_s^{00} - \chi_s^{02} m_{\pi}^{-2} \omega^2, \end{aligned} \quad (23)$$

$$\begin{aligned} \hat{H}_p^0 &= \nabla \frac{\chi_{p,1}^-(m_{\pi}) + \chi_{p,1}^+(m_{\pi})}{2} \cdot \nabla \\ &\equiv \nabla \chi_p^0 \cdot \nabla \approx \nabla \frac{4\pi c_0(m_{\pi}) \rho / \eta}{1 + 4\pi g' c_0(m_{\pi}) \rho / \eta} \cdot \nabla, \end{aligned} \quad (24)$$

$$\Delta \hat{H}_s = -\tilde{b}_1 \delta \rho m_{\pi}^{-1} \omega \equiv -\Delta \chi_s m_{\pi}^{-1} \omega, \quad (25)$$

$$\Delta \hat{H}_p = -\frac{2\pi\omega}{m_N \eta} c_1(m_{\pi}) (\nabla^2 \delta \rho) \equiv -\Delta \chi_p m_{\pi}^{-1} \omega. \quad (26)$$

### 2.3 Medium-modified Lagrangian

Evidently the explicit expressions of the self energies in configuration space follow from the standard rules  $\hat{H}^0(\omega) \rightarrow \hat{H}^0(i\partial_0)$  and  $\Delta \hat{H}(\omega) \rightarrow \Delta \hat{H}(i\partial_0)$ . After inserting the polarization operators  $\Pi(i\partial_0)$  and  $\Delta \Pi(i\partial_0)$  from (23)-(26) into the Lagrangian (11) and integrating by part, in order

<sup>2</sup> Within the framework of the Skyrme model, this situation corresponds to nucleons with  $S = T = \frac{1}{2} \sim \omega \Lambda$ , where  $\Lambda \approx 1$  fm is the moment of inertia of the skyrmion. In the case of  $\Delta$ -isobar states ( $S = T = \frac{3}{2} \sim \omega \Lambda$ ) also  $\omega^n$  terms with  $n \geq 3$  have to be taken into account.

to symmetrize in the time derivatives, one arrives at the final form of the medium-modified Lagrangian:

$$\mathcal{L}^* = \mathcal{L}_{\text{sym}}^* + \mathcal{L}_{\text{as}}^*, \quad (27)$$

$$\mathcal{L}_{\text{sym}}^* = \mathcal{L}_2^* + \mathcal{L}_4 + \mathcal{L}_{\chi\text{SB}}^*, \quad (28)$$

$$\mathcal{L}_{\text{as}}^* = \Delta\mathcal{L}_{\text{mes}} + \Delta\mathcal{L}_{\text{env}}^*, \quad (29)$$

$$\mathcal{L}_2^* = \frac{F_\pi^2}{16} \left\{ (1 + m_\pi^{-2} \chi_s^{02}) \text{Tr}(\partial_0 U \partial_0 U^\dagger) - (1 - \chi_p^0) \text{Tr}(\nabla U \cdot \nabla U^\dagger) \right\}, \quad (30)$$

$$\mathcal{L}_{\chi\text{SB}}^* = -\frac{F_\pi^2 m_\pi^2}{16} (1 + m_\pi^{-2} \chi_s^{00}) \times \text{Tr}[(U - 1)(U^\dagger - 1)], \quad (31)$$

$$\Delta\mathcal{L}_{\text{mes}} = -\frac{F_\pi^2}{16} \sum_{a=1}^2 \mathcal{M}_-^2 \text{Tr}(\tau_a U) \text{Tr}(\tau_a U^\dagger), \quad (32)$$

$$\Delta\mathcal{L}_{\text{env}}^* = -\frac{F_\pi^2}{16} \sum_{a,b=1}^2 \varepsilon_{ab3} (2m_\pi)^{-1} (\Delta\chi_s + \Delta\chi_p) \times \text{Tr}(\tau_a U) \text{Tr}(\tau_b \partial_0 U^\dagger). \quad (33)$$

Here  $\Delta\mathcal{L}_{\text{mes}}$  and  $\Delta\mathcal{L}_{\text{env}}^*$  are the isospin-breaking terms arising from the explicit symmetry breaking in the mesonic sector and the isospin asymmetry of the surrounding environment, respectively.

Note that both the temporal part of  $\mathcal{L}_2^*$  and the chiral symmetry breaking term  $\mathcal{L}_{\chi\text{SB}}^*$ , decrease – at leading order linearly – with increasing matter density, since  $\chi_s^{02}$  and  $\chi_s^{00}$  are negative, see Eqs. (20) and (23). However, as the same equations indicate,  $\chi_s^{02} \approx \chi_s^{00} \approx \tilde{b}_0 \rho$ , such that the effective mass, determined by the mass pole of the in-medium propagator, is approximately density-independent in agreement with the findings about the in-medium Gell-Mann–Oakes–Renner relation of Refs. [45, 46]. Furthermore, one can see that the Lagrangian (33) contains the Weinberg–Tomozawa term, as the relation

$$\frac{\Delta\chi_s}{4\pi\eta} = -\frac{m_\pi \delta\rho}{8\pi\eta f_{\pi,\text{ph}}^2} = b_1^{\text{l.o.}} \delta\rho \quad (34)$$

is based on the isovector  $s$ -wave scattering length in the chiral expansion to lowest order [51, 52].

The Lagrangian (27)–(33) will be used in our studies of isospin breaking effects in asymmetric nuclear matter. In the next sections we will present and discuss the changes that emerge due to the isospin asymmetry of the surrounding nuclear environment. Specifically, we will concentrate on isospin-breaking effects in infinite nuclear matter with a constant density, so that the  $p$ -wave contribution proportional to  $\Delta\chi_p \sim \nabla^2 \delta\rho$  vanishes. Note that in the case of finite nuclei this term may be essential for nucleons located near the surface of the nucleus.

### 3 Classical solitonic solutions

By following the two-stage method of Ref. [35]<sup>3</sup> of constrained and unconstrained collective isospin-rotations, applied to the hedgehog ansatz  $U = \exp[i\tau \cdot (\mathbf{r}/r)F(r)]$ , the time-dependent Lagrangian can be constructed from Eq. (27) in terms of the standard angular velocities  $\omega_i$  of the collective modes and the constrained angular velocity  $a^*$  (see below) as

$$L^* = \int \mathcal{L}^* d^3r = -M_{\text{NP}}^* - \mathcal{M}_-^2 \Lambda_- + \frac{\omega^2}{2} A^* + \omega_3 (a^* A^* + \Delta^*) + a^* \left( \frac{a^*}{2} A^* + \Delta^* \right). \quad (35)$$

Here

$$M_{\text{NP}}^* = \pi \int_0^\infty \left\{ \frac{F_\pi^2}{2} (1 - \chi_p^0) \left( F_r^2 + \frac{2S^2}{r^2} \right) + \frac{2}{e^2} \left( 2F_r^2 + \frac{S^2}{r^2} \right) \frac{S^2}{r^2} + F_\pi^2 (m_\pi^2 + \chi_s^{00}) (1 - \cos F) \right\} r^2 dr \quad (36)$$

is the in-medium mass of the soliton when it is not perturbed (NP) by any isospin breaking. The abbreviations  $F_r \equiv dF/dr$  and  $S \equiv \sin F$  have been used, where  $F = F(r)$  is the chiral profile function of the hedgehog ansatz. Furthermore

$$\Lambda^* = (1 + m_\pi^{-2} \chi_s^{02}) \Lambda_- + \Lambda_4 \quad (37)$$

with the separate contributions

$$\Lambda_- = \frac{2\pi}{3} F_\pi^2 \int_0^\infty S^2 r^2 dr, \quad (38)$$

$$\Lambda_4 = \frac{8\pi}{3e^2} \int_0^\infty \left( F_r^2 + \frac{S^2}{r^2} \right) S^2 r^2 dr \quad (39)$$

is the in-medium moment-of-inertia, whereas

$$\Delta^* = (2m_\pi)^{-1} \Delta\chi_s \Lambda_- \quad (40)$$

is the response of the isospin-asymmetric environment (see Eqs. (25) and (33)) to the collective iso-rotations.

The constrained angular velocity parameter  $a^*$  corresponds to a stationary rotation around the third axis in isotopic space that serves to undo the effect of the mesonic isospin-breaking term proportional to  $\mathcal{M}_-$  at the classical level, when the collective rotational modes in the isospin-space are frozen ( $\omega_{1,2,3} \rightarrow 0$ ). In this classical limit, applying the constraint [35]

$$a^{*2} = 2\mathcal{M}_-^2 \Lambda_- / A^*, \quad (41)$$

<sup>3</sup> An alternative, but equivalent way of introducing this method is presented in Appendix A.

one generates the Lagrangian

$$L^* = -M_{\text{NP}}^* + a^* \Delta^*. \quad (42)$$

The pertinent equation of motion for the hedgehog profile function  $F(r)$  takes then the form

$$\begin{aligned} & F_\pi^2 (1 - \chi_p^0) (r^2 F_{rr} + 2r F_r - S_2) \\ & + \frac{4}{e^2} \left[ 2S^2 F_{rr} + S_2 \left( F_r^2 - \frac{S^2}{r^2} \right) \right] \\ & - F_\pi^2 (m_\pi^2 + \chi_s^{00}) S r^2 + a^* \frac{F_\pi^2 \Delta \chi_s}{3m_\pi} S_2 r^2 = 0, \end{aligned} \quad (43)$$

where the additional abbreviations  $S_2 = \sin 2F$  and  $F_{rr} = d^2 F/dr^2$  were introduced.

The solution corresponding to the soliton of baryon number  $B = 1$  fulfills the boundary conditions

$$\lim_{r \rightarrow 0} F(r) = \pi - Cr, \quad (44)$$

$$\lim_{r \rightarrow \infty} F(r) = D (1 + m_\beta r) \exp \{-m_\beta r\} / r^2, \quad (45)$$

$$m_\beta^2 = \frac{m_\pi^2 + \chi_s^{00} - 2a^* m_\pi^{-1} \Delta \chi_s / 3}{1 - \chi_p^0}, \quad (46)$$

where  $C$  and  $D$  are constants. Since the parameter  $a^*$  is part of the classical equation (43), *i.e.*  $h(F_{rr}, F_r, F, a^*) = 0$ , this equation together with the constraint (41) can be solved by iteration:<sup>4</sup>

$$\begin{aligned} h(F_{rr}^{(0)}, F_r^{(0)}, F^{(0)}, 0) = 0 & \Rightarrow a_0^* = a^*(F_r^{(0)}, F^{(0)}); \\ h(F_{rr}^{(n)}, F_r^{(n)}, F^{(n)}, a_{n-1}^*) = 0 & \Rightarrow a_n^* = a^*(F_r^{(n)}, F^{(n)}). \end{aligned}$$

In the actual calculation, this iteration scheme rapidly converges after 3 to 4 iteration steps.

## 4 In-medium neutron-proton mass difference

### 4.1 Strong part of $\Delta m_{\text{np}}^*$

By taking into account the condition (41), applying the definition  $a_{\text{eff}}^* \equiv a^* + \Delta^*/\Lambda^*$  and using the canonical quantization procedure as in Ref. [35], one can construct from the Lagrangian (35) the Hamiltonian in terms of the isospin operator  $\hat{T}$ :

$$\begin{aligned} \hat{H}^* &= M_{\text{NP}}^* + \frac{\hat{T}_1^2}{2\Lambda^*} + \frac{\hat{T}_2^2}{2\Lambda^*} + \frac{(\hat{T}_3 - \Lambda^* a_{\text{eff}}^*)^2}{2\Lambda^*} \\ &= M_{\text{NP}}^* + \frac{\hat{T}^2}{2\Lambda^*} - a_{\text{eff}}^* \hat{T}_3 + \Lambda^* \frac{(a_{\text{eff}}^*)^2}{2}. \end{aligned} \quad (47)$$

Thus the strong part of the neutron-proton mass difference can be identified as

$$\Delta m_{\text{np}}^{*(\text{strong})} = a_{\text{eff}}^* = a^* + \frac{\Delta^*}{\Lambda^*}. \quad (48)$$

<sup>4</sup> The choice of the sign of  $a^*$  is fixed by the sign of  $\Delta m_{\text{np}}^{\text{strong}}$  in free space [35].

Note that the density-variation of the strong part of the neutron-proton mass difference will be more pronounced than in Ref. [35] for the following reasons: (i) the explicit density-dependence of the moment of inertia  $\Lambda^*$  (see Eq. (37)) resulting from the energy-dependent parameterization of the optical potentials, and (ii) the existence of the additional term  $\Delta^*/\Lambda^*$  in an isospin-asymmetric environment. Even if the explicit isospin breaking in the mesonic sector were omitted,  $\mathcal{M}_- = 0$ , there still would be a non-vanishing neutron-proton mass splitting proportional to the isospin-asymmetric environment factor  $\Delta^*$ .

### 4.2 Electromagnetic part of $\Delta m_{\text{np}}^*$

As discussed in Appendix B, by calculating the pertinent Noether currents one can construct the following isoscalar (S) and isovector (V) electromagnetic (EM) form factors

$$G_{\text{E}}^{\text{S}*}(\mathbf{q}^2) = \int_0^\infty \left( \frac{\tilde{B}}{2} - \frac{\Delta^*}{\Lambda^*} \tilde{A} + \tilde{A}^* \right) j_0(qr) dr, \quad (49)$$

$$G_{\text{M}}^{\text{S}*}(\mathbf{q}^2) = \frac{m_{\text{N}}(1 + \Delta^*)}{2\Lambda^*} \int_0^\infty \tilde{B} r^2 \frac{j_1(qr)}{qr} dr, \quad (50)$$

$$G_{\text{E}}^{\text{V}*}(\mathbf{q}^2) = \frac{1}{2\Lambda^*} \int_0^\infty \tilde{A}^* j_0(qr) dr, \quad (51)$$

$$G_{\text{M}}^{\text{V}*}(\mathbf{q}^2) = m_{\text{N}} \int_0^\infty \left[ (1 - \chi_p^0) \tilde{A}_- + \tilde{A}_4^* \right] \frac{j_1(qr)}{qr} dr, \quad (52)$$

in terms of the spherical Bessel functions  $j_0$  and  $j_1$  and the three-momentum transfer  $q = |\mathbf{q}|$ . Here a quantity with a tilde, say  $\tilde{Z} = \tilde{Z}(F)$ , is defined as the integrand of the corresponding functional, *i.e.*:

$$Z[F] \equiv \int_0^\infty \tilde{Z}(F(r)) dr.$$

As usual,  $B = 1$  is the baryon charge, such that  $\tilde{B}(r) = 4\pi r^2 B^0(r)$ , where  $B^0(r) = -\sin^2 F F_r / (2\pi^2 r^2)$  is the baryon density of the skyrmion. The medium-dependent form factors of the proton and neutron are defined as

$$G_{\text{E,M}}^{(\text{p})*}(\mathbf{q}^2) = G_{\text{E,M}}^{\text{S}*}(\mathbf{q}^2) \pm G_{\text{E,M}}^{\text{V}*}(\mathbf{q}^2)$$

with the normalization conditions  $G_{\text{E}}^{\text{p}*}(0) = 1$ ,  $G_{\text{E}}^{\text{n}*}(0) = 0$ ,  $G_{\text{M}}^{\text{p}*}(0) = \mu_{\text{p}}^*$ ,  $G_{\text{M}}^{\text{n}*}(0) = \mu_{\text{n}}^*$ , where  $\mu_{\text{p}}^*$  and  $\mu_{\text{n}}^*$  are the magnetic moments of the in-medium proton and neutron, respectively.

In the present approach all form factors *explicitly* depend on medium functionals, on the one hand, via the density-dependent moment of inertia  $\Lambda^*$  (see Eq. (37)), and on the other hand, via additional terms resulting from the isospin-asymmetric nuclear environment. Moreover, note the additional terms in the isoscalar form factors as compared with Ref. [35], which emerge here from

that part of the isospin charge density that is independent of the isospin  $T_3$  (see Appendix B).

Finally, applying the formula [53]

$$\Delta m_{np}^{*(\text{EM})} = -\frac{4\alpha}{\pi} \int_0^\infty dq \left\{ G_E^{S*}(q^2) G_E^{V*}(q^2) - \frac{q^2}{2m_N^2} G_M^{S*}(q^2) G_M^{V*}(q^2) \right\}, \quad (53)$$

where  $\alpha \approx 1/137$  is the fine-structure constant, one can calculate the medium-dependent electromagnetic part of the neutron-proton mass difference as in Ref. [35].

## 5 Results and discussions

In Fig. 1 the strong part of the in-medium neutron-proton mass splitting,  $\Delta m_{np}^{*(\text{strong})}$ , is shown for isospin-symmetric nuclear matter (solid curve), neutron-rich matter (dashed curve), pure neutron matter (dotted curve), and proton-rich matter (dot-dashed curve). Already in isospin-symme-

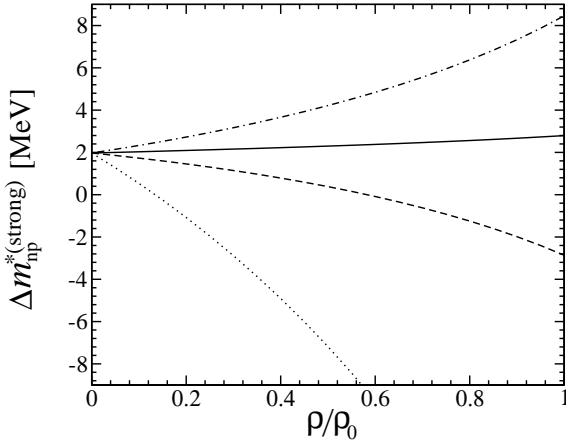


**Fig. 1.** Density dependence of the strong part  $\Delta m_{np}^{*(\text{strong})}$  of the neutron-proton mass difference. The abscissa represents the density  $\rho$  normalized to the saturation density of ordinary nuclear matter  $\rho_0 = 0.5m_\pi^3$ , while the ordinate shows the mass difference in units of MeV. The result in isospin-symmetric matter is plotted as a solid curve, the result of neutron-rich matter with  $\delta\rho/\rho = 0.2$  as dashed curve, the dotted curve represents pure neutron matter ( $\delta\rho/\rho = 1$ ) and the dot-dashed curve proton-rich matter with  $\delta\rho/\rho = -0.2$ .

tric matter  $\Delta m_{np}^{*(\text{strong})}$  has visibly a different density-behavior than the corresponding quantity of Ref. [35]. For example, at normal nuclear matter density,  $\Delta m_{np}^{*(\text{strong})}$  has increased by about 42% relative to its free space value (see the solid curve of Fig. 1). In contrast to this in the previous work [35], where the optical potentials were assumed to be energy-independent,  $\Delta m_{np}^{*(\text{strong})}$  decreased by a very tiny amount, namely by about 2% at normal

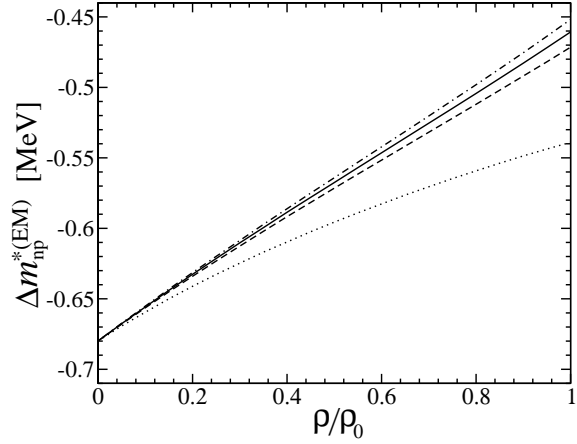


**Fig. 2.** Density dependence of the electromagnetic part  $\Delta m_{np}^{*(\text{EM})}$  of the neutron-proton mass difference. The axes and curves are defined as in Fig. 1.

nuclear matter densities; in other words,  $\Delta m_{np}^{*(\text{strong})}$  in Ref. [35] was practically density-independent.

Moreover, when the isospin symmetry of nuclear matter is broken,  $\delta\rho/\rho \neq 0$ ,<sup>5</sup>  $\Delta m_{np}^{*(\text{strong})}$  strongly varies at the qualitative as well as quantitative level (see the dashed curve in Fig. 1). In pure neutron matter the change becomes very drastic (see the dotted curve in Fig. 1), and  $\Delta m_{np}^{*(\text{strong})}$  decreases very fast with increasing density.

In contrast to the strong part, the electromagnetic part of the neutron-proton mass difference varies only by a small amount when the isospin-asymmetry parameter is increased (see Fig. 2). But compared with the result of the previous approach [35], the change is sizable, even in isospin-symmetric matter. This is again due to the explicit density dependence of the moment of inertia (37), and the changes in the solutions of the classical equations (43). Note that with increasing density the moment of inertia  $\Lambda^*$  decreases since  $\chi_s^{02} < 0$ . In addition, the solutions of the classical equations (43) are altered because  $\chi_s > 0$  in Eq. (22) of Ref. [35] is replaced by the  $\omega$ -independent part of the present Eq. (23), namely by  $\chi_s^{00}$  which is negative.

For completeness, we present the total neutron-proton mass difference in Fig. 3. From a comparison with Fig. 1 it is obvious that this mass difference is completely dominated by its strong part. In pure neutron matter and at the density  $\rho_0$ , the neutron-proton mass difference is  $\Delta m_{np}^* = -25$  MeV. For comparison, the authors of the work [11] got the result  $\Delta m_{np}^* \approx -70$  MeV in framework of QCD sum rule studies.

Another interesting result is the difference between the values of  $\Delta m_{np}^*$  in neutron-rich and proton-rich matter – compare the dashed and dash-dotted curves in Fig. 3. One can see that in neutron-rich matter  $\Delta m_{np}^*$  is decreased relative to the isospin-symmetric case, whereas in proton-rich matter the behavior is just opposite. This finding may become useful for future studies of mirror nuclei and their

<sup>5</sup> This quantity may be called the isospin-asymmetry parameter of the nuclear environment.

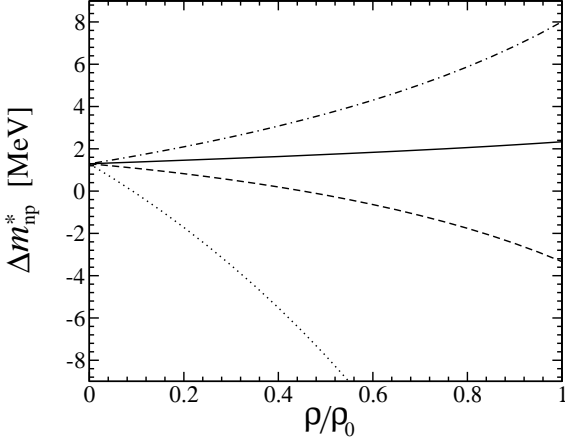


**Fig. 3.** Density dependence of the total neutron-proton mass difference  $\Delta m_{np}^*$ . The axes and curves are defined as in Fig. 1.

properties. For example, for the case of the mirror nuclei  $^{48}\text{Ca}$  and  $^{48}\text{Ni}$ , a similar behavior of  $\Delta m_{np}^*$  was found in Ref. [30] within density-dependent relativistic hadron field theory. The result of our work is also consistent with the findings of Refs. [23, 24, 25, 26, 27, 28, 29] that utilize a relativistic approach and with the nonrelativistic calculation [21] based on Skyrme-like effective interactions.

Even at the qualitative level, the various models mentioned in the introduction differ in their predictions of the neutron-proton mass difference in nuclear matter: (i) in nonrelativistic approaches [18, 19, 20], which are focused on the system properties as a whole, this difference mainly turns out to be positive ( $\Delta m_{np}^* > 0$ ); (ii) however, it is negative ( $\Delta m_{np}^* < 0$ ) in relativistic approaches [23, 24, 25, 26, 27, 28, 29] and some nonrelativistic variational calculations [21] or it becomes negative with increasing density in QCD sum rule studies [9, 10, 11]; (iii) it depends on the isospin content of the system ( $\Delta m_{np}^* > 0$  or  $\Delta m_{np}^* < 0$ ) in relativistic hadron field theory [30]. The effective masses in relativistic approaches are discussed in detail in Ref. [54]. Furthermore, the difference in the behavior of  $\Delta m_{np}^*$  in the relativistic and nonrelativistic approaches is explained in Ref. [24].

Also our approach shows that  $\Delta m_{np}^*$  qualitatively depends on the isospin content of surrounding environment. It is always positive in proton-rich matter as well as in isospin-symmetric matter (see the solid and dot-dashed curves in Fig. 3). In neutron-rich matter, however, the sign may change. For the reader's convenience, we plot in Fig. 4 those values of the density  $\rho$  as function of the isospin-asymmetry parameter  $\delta\rho/\rho$  where the in-medium neutron-proton mass splitting or its strong part vanishes. In other words the solutions of the 2-parameter equations,  $\Delta m_{np}^*(\rho, \delta\rho) = 0$  and  $\Delta m_{np}^{*(\text{strong})}(\rho, \delta\rho) = 0$ , are presented. For small positive input for the isospin-asymmetry parameter the neutron-proton mass difference or its strong part vanishes at high densities (of the order of the ordinary nuclear matter density  $\rho_0$ ). With increasing  $\delta\rho/\rho$ , however, the mass difference changes its sign at moder-

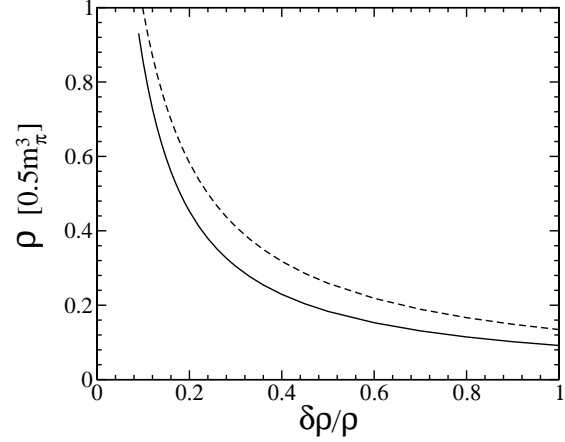


**Fig. 4.** The solutions of the 2-parameter equations  $\Delta m_{np}^*(\rho, \delta\rho) = 0$  and  $\Delta m_{np}^{*(\text{strong})}(\rho, \delta\rho) = 0$ . The abscissa represents the isospin-asymmetry parameter, while the ordinate shows the density (in units of the ordinary nuclear matter density  $\rho_0 = 0.5m_\pi^3$ ), where the neutron-proton mass difference (solid curve) or its strong part (dashed curve) vanishes.

ate densities, and in strongly isospin-asymmetric matter this transition is already at low densities. For instance, in neutron-rich matter with the isospin-asymmetry parameter  $\delta\rho/\rho \sim 0.1$  the proton becomes heavier at the density  $\rho \sim 0.85\rho_0$ . In pure neutron matter this change happens already at the density  $\rho \sim 0.09\rho_0$ .

In addition, in Table 1 we present the calculated effective masses and isoscalar as well as isovector charge radii of the in-medium nucleons for some values of the nuclear matter density.<sup>6</sup> In general, the nucleon masses strongly decrease in the nuclear medium and are qualitatively in agreement with the well known results [55, 56]. At normal nuclear matter density and for an isospin asymmetry  $\delta\rho/\rho \sim 0.25$ , the difference in the effective masses (normalized to the corresponding free space values) of the neutron and proton, respectively, is  $m_n^*/m_n - m_p^*/m_p \sim 0.01$ . For comparison, the result of Ref. [30] for nucleons located near the center of  $^{132}\text{Sn}$  is one order of magnitude bigger:  $m_n^*/m_n - m_p^*/m_p \sim 0.1$ .

The isoscalar and isovector charge radii  $\langle r^2 \rangle_{E,I=0,1}^{*1/2}$  increase with increasing density of the medium.<sup>7</sup> The isoscalar electric radius is more strongly affected by the isospin asymmetric environment than the isovector one because of the presence of the isospin breaking term  $\Delta^*$  (see appendix B). Consequently, in proton-rich matter the ratio  $\langle r^2 \rangle_{E,I=0}^{*1/2} / \langle r^2 \rangle_{E,I=0}^{1/2}$  is more enhanced than in neutron-rich matter.

<sup>6</sup> Note that the tabulated values of the free proton and neutron mass differ from their PDG values [43] since the customary Skyrme value  $M_N = 938 \text{ MeV}$  was used here and in Ref. [35] as input for the isospin-averaged nucleon mass.

<sup>7</sup> Note that our results in free space differ from the ones of Ref. [57] by a factor  $\sqrt{2}$  due to different normalizations of the charge densities (see Eq. (B.3) in the Appendix B and the corresponding definitions in Ref. [57]).

**Table 1.** Calculated masses (in units of MeV) and isoscalar as well as isovector charge radii (in units of fm) of the nucleons in nuclear matter of density  $\rho$  (in units of the saturation density of ordinary nuclear matter  $\rho_0 = 0.5m_\pi^3$ ).

$\rho/\rho_0$	$m_p^*$	$m_n^*$	$\langle r^2 \rangle_{E,I=0}^{*1/2}$	$\langle r^2 \rangle_{E,I=1}^{*1/2}$
In free space				
0	937.4	938.7	0.49	0.74
In proton-rich matter ( $\delta\rho/\rho = -0.2$ )				
0.5	729.6	733.3	0.61	0.84
1.0	547.9	555.9	0.79	0.98
In isospin symmetric matter ( $\delta\rho/\rho = 0$ )				
0.5	729.7	731.4	0.60	0.84
1.0	547.9	550.2	0.75	0.98
In neutron-rich matter ( $\delta\rho/\rho = 0.2$ )				
0.5	731.5	731.3	0.58	0.84
1.0	553.4	550.0	0.72	0.98
In pure neutron matter ( $\delta\rho/\rho = 1$ )				
0.5	757.9	750.1	0.54	0.83
1.0	632.1	607.0	0.52	0.94

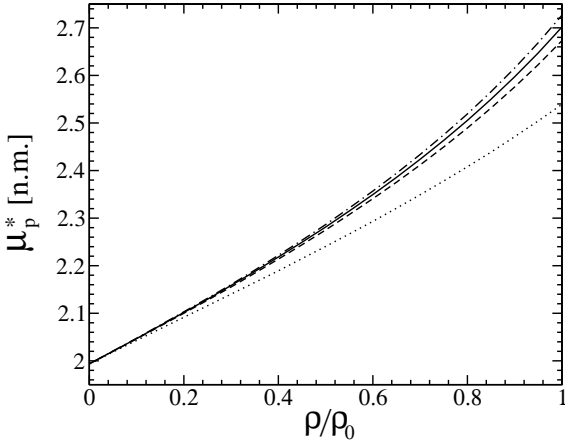


**Fig. 5.** Density dependence of the proton magnetic moment. The ordinate represents  $\mu_p^*$  in nuclear Bohr magnetons (n.m.). The other definitions are as in Fig. 1.

The density-dependence of the magnetic moments of the in-medium proton and the neutron is presented in Fig. 5 and Fig. 6, respectively. The influence of the isospin asymmetry of the surrounding environment on the in-medium magnetic moments is comparatively weak in this case. Relative to the result in isospin-symmetric matter both, the proton and neutron magnetic moments are decreased in neutron-rich matter and increased in proton-rich matter.

Let us conclude by remarking that within the present approach the change of  $\Delta m_{np}^*$  is completely dictated by its strong part when the isospin-asymmetry parameter is sizable (compare Figs. 1, 2 and 3).

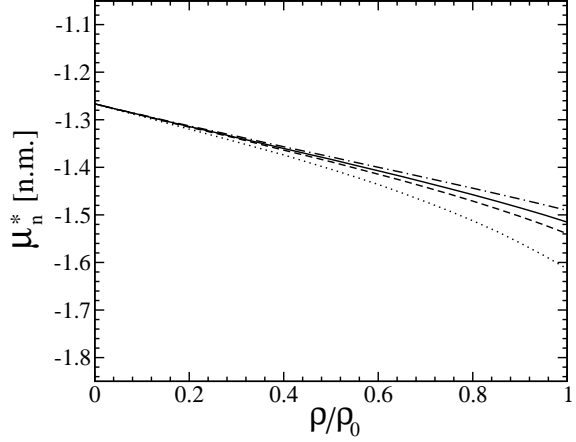


**Fig. 6.** Density dependence of the neutron magnetic moment. The ordinate represents  $\mu_n^*$  in nuclear Bohr magnetons (n.m.). The other definitions are as in Fig. 1.

## 6 Summary and outlook

We have proposed an effective Lagrangian which incorporates energy-dependent optical potentials for the  $s$ - and  $p$ -waves and which takes into account the influence of the isospin-asymmetry of the environment onto the Skyrme-solitons of the model. As a result the neutron-proton mass splitting in asymmetric nuclear matter is predicted to vary strongly relative to its free space value. The predictions obtained in the present work are in a qualitative agreement with the ones obtained within relativistic hadron field theory [28, 29, 30] and nonrelativistic variational calculations [21]. Quantitatively, however, the changes of  $\Delta m_{np}^*$  are small in comparison to the results of those works. Our approach shows that  $\Delta m_{np}^*$  in nuclear matter with sizable asymmetry is mainly dictated by its strong part. In the case of more complicated calculations involving finite nuclei this may serve as a justification to evaluate only the strong part of the mass difference within the present approach.

Consequently, the next step in our future studies will be the estimate of  $\Delta m_{np}^*$  in finite (particularly in mirror) nuclei. Here additional effects are expected because the  $p$ -wave contribution proportional to  $\Delta\chi_p \sim \nabla^2\delta\rho$  in the Lagrangian (33) and the deformation effects discussed in Refs. [58, 59] become relevant.

The work of U.T.Y. was supported by the Alexander von Humboldt Foundation. Partial financial support from the EU Integrated Infrastructure Initiative Hadron Physics Project (contract number RII3-CT-2004-506078), by the DFG (TR 16, “Subnuclear Structure of Matter”) and by BMBF (research grant 06BN411) is gratefully acknowledged.

## A Two-stage method and classical solutions

In this appendix we review a new interpretation for the inclusion of the stationary  $a^*$  rotations that is different



from the one of Ref. [36] or the one of Ref. [35], but which leads – under the same input – to the same results as in those references. This new strategy is more convenient for our analytic calculations.

First of all we remark that stationary  $a^*$  rotations essentially have to be introduced because of the explicit isospin breaking in the mesonic sector, *i.e.* when  $\mathcal{M}_- \neq 0$ . If  $\mathcal{M}_- = 0$  then  $a^* = 0$ . Of course, the condition (41) satisfies this requirement. Secondly, at the classical level, at which the soliton solution is determined, this mesonic mass splitting can be ignored – at the quantum level, however, this can not be the case since the symmetry breaking effect is enhanced by the coupling to the collective zero modes. Note the quadratic dependence on the small parameter  $\mathcal{M}_-$  at the classical level, whereas at the quantum level the dependence is linear; compare Eq. (41) with Eq. (47).

Let us, for the moment, put  $\mathcal{L}_{\text{as}}^* = 0$  in the Lagrangian (27). Then one can construct the classical ‘hedgehog’ solution(s) from the static Lagrangian  $\mathcal{L}_{\text{sym}}^{*(\text{static})}$ . In the work [35] these solutions are referred to as the solutions of the non-perturbed (NP) system, determined by

$$\frac{\delta M_{\text{NP}}^*[F]}{\delta F} = 0, \quad (\text{A.1})$$

where  $F(r)$  is the usual chiral profile function of the hedgehog ansatz and where  $M_{\text{NP}}^* = -\int \mathcal{L}_{\text{sym}}^{*(\text{static})} d^3r$  (compare with Eq. (35)) is the in-medium mass of the soliton when it is not perturbed by any isospin breaking. The Lagrangian  $\mathcal{L}_{\text{sym}}^{*(\text{static})}$  is invariant under time-independent isospin rotations

$$U \rightarrow AUA^\dagger, \quad A = \exp\{i\boldsymbol{\tau} \cdot \boldsymbol{\varphi}^I/2\}, \quad (\text{A.2})$$

which can be treated as the usual zero modes of the model. The resurrection of the time dependence  $\boldsymbol{\varphi}^I \rightarrow \boldsymbol{\varphi}^I(t)$  in Eq. (A.2) leads to the (spatially integrated) Lagrangian

$$\int \mathcal{L}_{\text{sym}}^* d^3r = -M_{\text{NP}}^* + \frac{(\dot{\boldsymbol{\varphi}}^I(t))^2}{2} \Lambda^*,$$

where  $\Lambda^*$  is the in-medium moment-of-inertia.

Now we plug the isospin breaking  $\mathcal{M}_- \neq 0$  back into the mesonic sector, such that the corresponding Lagrangian reads

$$\int d^3r \left\{ \mathcal{L}_{\text{sym}}^* + \Delta \mathcal{L}_{\text{mes}} \right\} = -M_{\text{NP}}^* + \frac{(\dot{\boldsymbol{\varphi}}^I(t))^2}{2} \Lambda^* - \mathcal{M}_-^2 \Lambda_- . \quad (\text{A.3})$$

Note that the integrated Lagrangian (A.3), even in the presence  $\mathcal{M}_- \neq 0$ , is still invariant under additional time-independent isospin rotations, *e.g.*

$$\begin{aligned} A(t) &\rightarrow \tilde{A}(t) = \exp\{i\boldsymbol{\tau} \cdot [\boldsymbol{\varphi}^I(t) + \boldsymbol{\varphi}^{II}]/2\} \\ &\equiv \exp\{i\boldsymbol{\tau} \cdot \boldsymbol{\varphi}(t)/2\}. \end{aligned} \quad (\text{A.4})$$

In fact, it is a property of the hedgehog ansatz that these time-independent isospin rotations can be compensated by time-independent spatial rotations. The latter average

out when the angular integration is performed, although  $\mathcal{M}_- \neq 0$ . But in order to be consistent in the use of the *unchanged* classical solution  $F(r)$  determined by Eq. (A.1), one has to introduce – at the classical level – the requirement

$$\frac{(\dot{\boldsymbol{\varphi}}^I)^2}{2} \Lambda^* - \mathcal{M}_-^2 \Lambda_- = 0. \quad (\text{A.5})$$

One can see explicitly that classically not all the rotations  $\varphi_1^I, \varphi_2^I, \varphi_3^I$  of Eq. (A.2) can be time-independent. In other words, at least one of the angular velocities  $\dot{\varphi}_1^I, \dot{\varphi}_2^I, \dot{\varphi}_3^I$  must not vanish, say, the one with respect to the third axis in isotopic space (which will later be the quantization axis). We will call the corresponding (via Eq. (A.5)) constrained angular velocity  $a^*$ , such that the condition (A.5) is nothing else than the constraint (41). As mentioned above, after angular averaging, the system remains invariant under time-independent zero modes which we called  $\varphi_1^{II}, \varphi_2^{II}, \varphi_3^{II}$ . Again these zero modes can be made time-dependent

$$\dot{\varphi}_1^{II} = \omega_1, \quad \dot{\varphi}_2^{II} = \omega_2, \quad \dot{\varphi}_3^{II} = \omega_3, \quad (\text{A.6})$$

where  $\omega_1, \omega_2, \omega_3$ , in contrast to  $a^*$ , are unconstrained angular velocities. Transcribed to our starting point (A.4), we eventually arrive at

$$\dot{\varphi}_1 = \omega_1, \quad \dot{\varphi}_2 = \omega_2, \quad \dot{\varphi}_3 = \omega_3 + a^*. \quad (\text{A.7})$$

Inserting  $\dot{\varphi}_1, \dot{\varphi}_2, \dot{\varphi}_3$  into Eq. (A.3) one generates the Lagrangian (35) with  $\Delta^* = 0$ . Interpreting now  $\phi_1 = \varphi_1, \phi_2 = \varphi_2, \phi_3 = \varphi_3 - a^*t$  as collective coordinates and  $\omega_1, \omega_2, \omega_3$  as their pertinent velocities, the standard quantization procedure should be performed around the stationary point  $a^*t$  with the constant angular velocity  $a^*$ .

This way of handling the classical  $a^*$  rotations is equivalent to the procedure performed in Refs. [35,36]. But there is no need anymore for the explicit introduction of the matrix  $\mathcal{T}(t)$  (see equation (15) in Ref. [35]) and the interpretation of the corresponding matrix order ambiguities discussed in Ref. [36].

Thus at the analytical level one performs the usual Skyrme model calculations, where Eq. (A.7) is inserted into the expression (A.3) and where the constraint (41) is applied at the classical level, such that  $L^* = -M_{\text{NP}}^*$  is extremized under the hedgehog ansatz, see Eq. (A.1). The latter corresponds to classical equation of motion (43) for the iso-symmetric matter case with vanishing  $\delta\rho$  and therefore, according to the definition (25), vanishing  $\Delta\chi_s$  (and vanishing  $\Delta^*$ , see Eq. (40)).

Finally, the inclusion of isospin-breaking effects due to the asymmetric environment ( $\Delta\mathcal{L}_{\text{env}}^* \neq 0$ ) leads to the Lagrangian

$$\begin{aligned} &\int d^3r \left\{ \mathcal{L}_{\text{sym}}^* + \Delta \mathcal{L}_{\text{mes}} + \Delta \mathcal{L}_{\text{env}}^* \right\} \\ &= -M_{\text{NP}}^* + \frac{(\dot{\boldsymbol{\varphi}})^2}{2} \Lambda^* - \mathcal{M}_-^2 \Lambda_- + \dot{\varphi} \Delta^*. \end{aligned} \quad (\text{A.8})$$

Note that the Lagrangian (A.8), because of the angular averaging, remains invariant under time-independent

isospin-rotations as its counterpart (A.3). The collective coordinates are therefore  $\phi_1 = \varphi_1, \phi_2 = \varphi_2, \phi_3 = \varphi_3 - a^*t$  as before and Eq. (A.7) is still valid. When the latter is inserted, Eq. (A.8) transforms to the Lagrangian (35) which is the starting point for the quantization in this work. But in order to be consistent with the use of a solution of hedgehog type, one still has to satisfy two requirements: (i) to apply the constraint (41) in order to remove  $-\mathcal{M}_-^2 \Lambda_-$  and  $\Lambda^*(\dot{\varphi})^2/2$  from (A.8), and (ii) to extremize the remainder  $-M_{\text{NP}}^* + \dot{\varphi}\Delta^*$  (compare with Eq. (42)) under the hedgehog ansatz. Here  $\dot{\varphi}(t)$  still corresponds to  $\dot{\varphi}^I(t) = a^*$ , *i.e.*  $\varphi^{II}$  is still assumed to be time-independent. Consequently, instead of Eq. (A.1) it is Eq. (43) with  $\Delta\chi_s \neq 0$  that has to be solved (in practice by iteration) in order to determine the profile function  $F(r)$ .

## B Charges and magnetic moments

In calculating the third component of the isospin current  $V_0^{(3)}$ , one finds

$$\int d^3r V_0^{(3)} = (\omega_3 + a^*)\Lambda^* + \Delta^* \equiv T_3. \quad (\text{B.1})$$

Consequently, the isospin charge *density* – modulo a factor  $4\pi r^2$  – is given as

$$\tilde{T}_3 = (\omega_3 + a^*)\tilde{\Lambda}^* + \tilde{\Delta}^* = (T_3 - \Delta^*)\frac{\tilde{\Lambda}^*}{\Lambda^*} + \tilde{\Delta}^*. \quad (\text{B.2})$$

Note that there are terms that are independent of the isospin  $T_3$  on the r.h.s. Since the charges of the nucleons are defined as

$$Q = \frac{B}{2} + T_3 \equiv \int \rho_{I=0}(r) d^3r \pm \int \rho_{I=1}(r) d^3r, \quad (\text{B.3})$$

the isoscalar and the isovector density distributions have here the following form

$$4\pi r^2 \rho_{I=0}(r) = \frac{\tilde{B}}{2} - \frac{\Delta^*}{\Lambda^*} \tilde{\Lambda}^* + \tilde{\Delta}^*, \quad (\text{B.4})$$

$$4\pi r^2 \rho_{I=1}(r) = \frac{\tilde{\Lambda}^*}{2\Lambda^*}. \quad (\text{B.5})$$

Analogous calculations for the magnetic moments lead to

$$\begin{aligned} \mu_{\left(\frac{p}{n}\right)^*} &= \frac{m_N(1 + \Delta^*)}{6\Lambda^*} \int_0^\infty \tilde{B} r^2 dr \\ &\pm \frac{m_N}{3} \int_0^\infty \left[ (1 - \chi_p^0) \tilde{\Lambda}_- + \tilde{\Lambda}_4^* \right] dr. \end{aligned} \quad (\text{B.6})$$

## References

1. B. A. Li, C. M. Ko and W. Bauer, Int. J. Mod. Phys. E **7**, 147 (1998) [arXiv:nucl-th/9707014].

2. V. Baran, M. Colonna, V. Greco and M. Di Toro, Phys. Rept. **410**, 335 (2005) [arXiv:nucl-th/0412060].
3. A. W. Steiner, M. Prakash, J. M. Lattimer and P. J. Ellis, Phys. Rept. **411**, 325 (2005) [arXiv:nucl-th/0410066].
4. G. Steigman, Int. J. Mod. Phys. E **15**, 1 (2006) [arXiv:astro-ph/0511534].
5. R. H. Cyburt, Phys. Rev. D **70**, 023505 (2004) [arXiv:astro-ph/0401091].
6. J. A. Nolen and J. P. Schiffer, Ann. Rev. Nucl. Part. Sci. **19**, 471 (1969).
7. P. J. Woods and C. N. Davids, Ann. Rev. Nucl. Part. Sci. **47**, 541 (1997).
8. J. Rizzo, M. Colonna, M. Di Toro and V. Greco, Nucl. Phys. A **732**, 202 (2004) [arXiv:nucl-th/0309032].
9. T. Hatsuda, H. Høgaasen and M. Prakash, Phys. Rev. C **42**, 2212 (1990).
10. T. Hatsuda, H. Høgaasen and M. Prakash, Phys. Rev. Lett. **66**, 2851 (1991) [Erratum-ibid. **69**, 1290 (1992)].
11. E. G. Drukarev, M. G. Ryskin and V. A. Sadovnikova, Phys. Rev. C **70**, 065206 (2004) [arXiv:nucl-th/0406027].
12. C. Adami and G. E. Brown, Z. Phys. A **340**, 93 (1991).
13. U.-G. Meißner and H. Weigel, Phys. Lett. B **267**, 167 (1991).
14. M. Fiolhais, C. Christov, T. Neuber, M. Bergmann and K. Goeke, Phys. Lett. B **269**, 43 (1991).
15. T. Schäfer, V. Koch and G. E. Brown, Nucl. Phys. A **562**, 644 (1993).
16. K. Saito and A. W. Thomas, Phys. Lett. B **335**, 17 (1994) [arXiv:nucl-th/9405009].
17. H. R. Christiansen, L. N. Epele, H. Fanchiotti and C. A. Garcia Canal, Phys. Rev. C **53**, 1911 (1996) [arXiv:hep-ph/9602244].
18. I. Bombaci and U. Lombardo, Phys. Rev. C **44**, 1892 (1991).
19. W. Zuo, I. Bombaci and U. Lombardo, Phys. Rev. C **60**, 024605 (1999) [arXiv:nucl-th/0102035].
20. W. Zuo, L. G. Cao, B. A. Li, U. Lombardo and C. W. Shen, Phys. Rev. C **72**, 014005 (2005) [arXiv:nucl-th/0506003].
21. E. Chabanat, J. Meyer, P. Bonche, R. Schaeffer and P. Haensel, Nucl. Phys. A **627**, 710 (1997).
22. T. Lesinski, K. Bennaceur, T. Duguet and J. Meyer, Phys. Rev. C **74**, 044315 (2006) [arXiv:nucl-th/0607065].
23. M. Lopez-Quelle, S. Marcos, R. Niembro, A. Bouyssy and V. G. Nguyen, Nucl. Phys. A **483**, 479 (1988).
24. E. N. E. van Dalen, C. Fuchs and A. Faessler, Phys. Rev. Lett. **95**, 022302 (2005) [arXiv:nucl-th/0502064].
25. E. N. E. van Dalen, C. Fuchs and A. Faessler, Phys. Rev. C **72**, 065803 (2005) [arXiv:nucl-th/0511040].
26. E. N. E. van Dalen, C. Fuchs and A. Faessler, Eur. Phys. J. A **31**, 29 (2007) [arXiv:nucl-th/0612066].
27. S. Kubis and M. Kutschera, Phys. Lett. B **399**, 191 (1997) [arXiv:astro-ph/9703049].
28. B. Liu, V. Greco, V. Baran, M. Colonna and M. Di Toro, Phys. Rev. C **65**, 045201 (2002) [arXiv:nucl-th/0112034].
29. V. Greco, M. Colonna, M. Di Toro, G. Fabbri and F. Matera, Phys. Rev. C **64**, 045203 (2001) [arXiv:nucl-th/0011033].
30. F. Hofmann, C. M. Keil and H. Lenske, Phys. Rev. C **64**, 034314 (2001) [arXiv:nucl-th/0007050].
31. K. Tsushima, K. Saito and A. W. Thomas, Phys. Lett. B **465**, 36 (1999) [arXiv:nucl-th/9907101].

32. L. W. Chen, C. M. Ko, B. A. Li and G. C. Yong, arXiv:0704.2340 [nucl-th].
33. T. H. R. Skyrme, Proc. Roy. Soc. Lond. A **260**, 127 (1961).
34. T. H. R. Skyrme, Nucl. Phys. **31**, 556 (1962).
35. U.-G. Meißner, A. M. Rakhimov, A. Wirzba and U. T. Yakhshiev, Eur. Phys. J. A **31**, 357 (2007) [arXiv:nucl-th/0611066].
36. E. Rathske, Z. Phys. A **331**, 499 (1988).
37. V. Bernard, N. Kaiser and U.-G. Meißner, Phys. Lett. B **309**, 421 (1993) [arXiv:hep-ph/9304275].
38. V. Bernard, N. Kaiser and U.-G. Meißner, Phys. Rev. C **52**, 2185 (1995) [arXiv:hep-ph/9506204].
39. N. Kaiser and W. Weise, Phys. Lett. B **512**, 283 (2001) [arXiv:nucl-th/0102062].
40. E. E. Kolomeitsev, N. Kaiser and W. Weise, Phys. Rev. Lett. **90**, 092501 (2003) [arXiv:nucl-th/0207090].
41. E. Friedman and A. Gal, Phys. Lett. B **578**, 85 (2004) [arXiv:nucl-th/0308030].
42. T. Ericson and W. Weise, *Pions and Nuclei* (Clarendon, Oxford, 1988).
43. W. M. Yao *et al.* [Particle Data Group], J. Phys. G **33**, 1 (2006).
44. J. Delorme, M. Ericson and T. E. O. Ericson, Phys. Lett. B **291**, 379 (1992).
45. V. Thorsson and A. Wirzba, Nucl. Phys. A **589**, 633 (1995) [arXiv:nucl-th/9502003]; A. Wirzba and V. Thorsson, arXiv:hep-ph/9502314.
46. U.-G. Meißner, J. A. Oller and A. Wirzba, Annals Phys. **297**, 27 (2002) [arXiv:nucl-th/0109026].
47. U.-G. Meißner, PoS **LAT2005**, 009 (2006) [arXiv:hep-lat/0509029].
48. H. C. Schröder *et al.*, Eur. Phys. J. C **21**, 473 (2001).
49. U.-G. Meißner, U. Raha and A. Rusetsky, Phys. Lett. B **639**, 478 (2006) [arXiv:nucl-th/0512035].
50. R. A. Arndt, W. J. Briscoe, R. L. Workman and I. I. Strakovsky, the SAID  $\pi N$  data base from <http://gwdac.phys.gwu.edu/>.
51. S. Weinberg, Phys. Rev. Lett. **17**, 616 (1966).
52. Y. Tomozawa, Nuovo Cim. **46A**, 707 (1966).
53. J. Gasser and H. Leutwyler, Phys. Rep. **87**, 77 (1982).
54. M. Jaminon and C. Mahaux, Phys. Rev. C **40**, 354 (1989).
55. J. P. Jeukenne, A. Lejeune and C. Mahaux, Phys. Rep. **25**, 83 (1976).
56. C. Mahaux, P. F. Bortignon, R. A. Broglia, and C. H. Dasso, Phys. Rep. **120**, 1 (1985).
57. G. S. Adkins and C. R. Nappi, Nucl. Phys. B **233**, 109 (1984).
58. U. T. Yakhshiev, M. M. Musakhanov, A. M. Rakhimov, U.-G. Meißner and A. Wirzba, Nucl. Phys. A **700**, 403 (2002) [arXiv:nucl-th/0109008].
59. U. T. Yakhshiev, U.-G. Meißner and A. Wirzba, Eur. Phys. J. A **16**, 569 (2003) [arXiv:nucl-th/0211055].